Partitioning, diffusion, and ligand binding of raft lipid analogs in model and cellular plasma membranes

Erdinc Sezgin [a,b], Ilya Levental [b], Michal Grzybek [b], Günter Schwarzmann [c], Veronika Mueller [d], Alf Honigmann [d], Vladimir N. Belov [d], Christian Eggeling [d], Ünal Coskun [b], Kai Simons [b], Petra Schwille [a,b,*]

[a] Biophysics/BIOTEC, TU Dresden, Tatzberg 47-51, 01307 Dresden, Germany
[b] Max Planck Institute for Molecular Cell Biology and Genetics, Pfotenhauerstrasse 108, 01307 Dresden, Germany
[c] LIMES Membrane Biology and Lipid Biochemistry Unit, University of Bonn, Gerhard-Domagk-Strasse 1, 53121 Bonn, Germany
[d] Max Planck Institute for Biophysical Chemistry, Department NanoBiophotonics, Am Fassberg 11, 37077, Göttingen, Germany

ARTICLE INFO

ABSTRACT

Several simplified membrane models featuring coexisting liquid disordered (Ld) and ordered (Lo) lipid phases have been developed to mimic the heterogeneous organization of cellular membranes, and thus, aid our understanding of the nature and functional role of ordered lipid–protein nanodomains, termed "rafts". In spite of their greatly reduced complexity, quantitative characterization of local lipid environments using model membranes is not trivial, and the parallels that can be drawn to cellular membranes are not always evident. Similarly, various fluorescently labeled lipid analogs have been used to study membrane organization and function in vitro, although the biological activity of these probes in relation to their native counterparts often remains uncharacterized. This is particularly true for raft-preferring lipids ("raft lipids", e.g. sphingolipids and sterols), whose domain preference is a strict function of their molecular architecture, and is thus susceptible to disruption by fluorescence labeling. Here, we analyze the phase partitioning of a multitude of fluorescent raft lipid analogs in synthetic Giant Unilamellar Vesicles (GUVs) and cell-derived Giant Plasma Membrane Vesicles (GPMVs). We observe complex partitioning behavior dependent on label size, polarity, charge and position, lipid headgroup, and membrane composition. Several of the raft lipid analogs partitioned into the ordered phase in GPMVs, in contrast to fully synthetic GUVs, in which most raft lipid analogs mis-partitioned to the disordered phase. This behavior correlates with the greatly enhanced order difference between coexisting phases in the synthetic system. In addition, not only partitioning, but also ligand binding of the lipids is perturbed upon labeling: while cholera toxin B binds unlabeled GM1 in the Lo phase, it binds fluorescently labeled GM1 exclusively in the Ld phase. Fluorescence correlation spectroscopy (FCS) by stimulated emission depletion (STED) nanoscopy on intact cellular plasma membranes consistently reveals a constant level of confined diffusion for raft lipid analogs that vary greatly in their partitioning behavior, suggesting different physicochemical bases for these phenomena.

© 2012 Elsevier B.V. All rights reserved.

1. Introduction

The minimal system approach aims to uncover the principles underlying biological processes by minimizing the number of variables, thus decreasing complexity, while retaining the functionality of the system [1]. For research on biological membranes, several minimal systems exist to study both isolated lipid behavior and the interplay of lipids and proteins [2]. Giant Unilamellar Vesicles (GUVs) are widely used model membranes [3–5] that have found a large variety of applications [6–12], due to their ease of preparation and strict control of membrane composition. Yet, having a limited number of components, GUVs cannot fully recapitulate many important properties of

cellular membranes, most notably due to the lack of leaflet asymmetry and membrane spanning proteins that comprise a major fraction of all biological membranes. An intermediate model system between fully synthetic GUVs and live cell membranes is giant plasma membrane vesicles (GPMVs), microscopic spheres of plasma membranes harvested from live cells following chemical treatment [13,14]. GPMVs resemble native biological membranes in lipid and protein diversity, but have the disadvantage of rather high compositional variation and complexity.

The most widely investigated physicochemical phenomenon of biomimetic membranes is the liquid–liquid phase coexistence occurring when saturated lipids and sterols condense to form a liquid ordered (Lo) phase, which separates from an unsaturated lipid-rich liquid disordered (Ld) phase. Lo/Ld phase separation in GUVs and GPMVs has been extensively characterized [6–12,15–21] and proposed as a physical basis underlying the raft concept in cell

* Corresponding author at: Biophysics/BIOTEC, TU Dresden, Tatzberg 47-51, 01307 Dresden, Germany. Tel.: +49 35 146340328.
E-mail address: schwille@biotec.tu-dresden.de (P. Schwille).

membranes [8,22,23]. This concept postulates the self-organization of certain molecules in cellular membranes into segregated lipid and protein nanodomains, which transiently concentrate specific proteins and lipids in an active and dynamic platform to take part in cellular processes such as membrane trafficking, signaling, etc. [24–32].

Measurements of membrane nanostructure require specific visualization of lipids and proteins, realized by adding a fluorescent label to the molecule of interest. The discovery of the green fluorescent protein (GFP) enabled direct observation of proteins both in their native environment and in the synthetic systems described above [16,17,33]. In the case of lipids, such a universal probe is not available. To sensitively and selectively probe the lipid environment [34,35], coupling synthetic fluorescent moieties to lipids and incorporating these analogs into cell membranes have become a common protocol for optical investigation of membranes, e.g. by fluorescent analogs of cholesterol [36–39], sphingomyelin [38,40–42], GM1 [40,43–45], PC, and PE [16]. However, there are important caveats that must be considered for the interpretation of these results. The molecular sizes of lipids and their fluorescence tags are usually of the same order (<2 kDa). In addition, the physicochemical properties of lipids (e.g. molecular shape, planarity, flexibility, and hydrophobicity) are deterministic of both their collective and individual behaviors in membranes. Thus, the addition of bulky tags, often containing hydrophilic groups, may drastically affect native lipid behavior [16]. This is particularly true of raft lipids (i.e. those that would be expected to enrich in raft domains based on their enrichment in detergent resistant membranes — sphingolipids, sterols, etc.), which require specific structural features to allow their condensation into an ordered domain. Correspondingly, apart from a few examples [46–48], most fluorescent raft lipid analogs do not enter the raft-mimetic Lo phase of model membranes [16,43,46,49–53].

As a complement to minimal membrane model systems, local heterogeneity in the membranes of live cells has been probed by measuring the diffusion of lipids and proteins (e.g. by single particle tracking (SPT) [54] and Fluorescence Correlation Spectroscopy (FCS) [6]) since the introduction of the raft hypothesis [22,55]. In contrast to SPT, where a labeled molecule is tracked with very high positional accuracy to reveal the local membrane structure, FCS on cellular membranes suffered from the relatively large size of the confocal observation spot compared to the size of putative lipid nanodomains. Recently, the addition of FCS to STED nanoscopy [56–58] (used to tune focal spots down to 30 nm in diameter) revealed transient local confinement of fluorescent sphingolipid and ganglioside (but not phosphoglycerolipid) analogs in the plasma membrane of living cells [40,59]. Despite the large difference in nanoscopic diffusion between fluorescent sphingo- and phosphoglycerolipids, both lipids have been shown to mainly partition into the Ld phase of model membranes [59,60]. Consequently, it remains to be shown how the transient nanoscopic interactions probed by STED-FCS relate to ordered phases in model membranes and functional rafts in live cells.

Due to the mis-partitioning of most fluorescent lipid analogs in model membranes, the justification of using GUVs as model systems and fluorescent lipid analogs as probes of heterogeneous membrane organization in vivo has been challenged. In this report, we extend previous observations and perform a systematic comparison of phase partitioning, diffusion and binding characteristics of a multitude of differently labeled and either commercially available or specifically synthesized raft lipid analogs in cellular and model membranes. We compare phase partitioning in fully synthetic GUVs and cell-derived GPMVs, and relate it to nanoscopic diffusion characteristics in the plasma membrane of living cells as measured by STED-FCS. We also study the influence of tagging the ganglioside GM1 with an organic dye on its ability to bind its native ligand, cholera toxin B (CTxB). We show that many of the fluorescent raft lipid probes partition to the raft-mimetic ordered phase in GPMVs, in contrast to GUVs. Moreover, we show that binding of GM1 to CTxB changes dramatically upon labeling. Finally, our data show that phase association of raft lipid analogs in model membranes does not correlate with confined diffusion measured by STED-FCS.

2. Materials and methods

2.1. Fluorescent probes

We labeled sphingomyelin (SM) and the ganglioside GM1 either at the headgroup (H) or at the water–lipid interface by replacing the native long acyl chain with a short acyl chain (AC) carrying the dye with different dyes: NBD, TopFluor (TF), Bodipy-FL (BD-FL), Bodipy-TMR (BD-TMR), Atto532, Atto647N and KK114 [61]. TF SM and NBD-C12 SM were purchased from Avanti Polar Lipids (AL, USA) and BD-FL labeled SM and GM1 and NBD-C6 SM from Invitrogen (CA, USA). NBD-C6 GM1 and the Atto532, Atto647N and KK114 labeled lipid analogs were synthesized as outlined previously [40,45,59,61,62]. The cholesterol analogs were purchased from Avanti (TF) or Invitrogen (BD-TMR). For the lipid dye structures refer to Supplementary Fig. 1. Fast DiO, Fast DiI and DiD C18 were purchased from Invitrogen (CA, USA) and Alexa647 or Alexa555 labeled cholera toxin B (CTxB) from Sigma-Aldrich (MO, USA). C-Laurdan was a gift from Dr. B. R. Cho (Seoul, Korea).

2.2. GUV preparation

For preparing Ld/Lo phase separated GUVs, dioleoyl phosphatidylcholine (DOPC), brain sphingomyelin (BSM), and cholesterol (Chol) (Avanti Polar Lipids) were mixed with a molar ratio of 2:2:1. The lipid analogs were added at 0.1–0.2 mol%. We usually added two lipid analogs: one analog whose partitioning characteristics are unknown and to be determined, and the membrane dye markers DiO, DiI or DiD, which are known to partition with a strong preference into the Ld phase of GUVs or GPMVs, i.e. they identify the Ld phase [15,16]. GUVs were prepared using platinum wires as described previously [63]. For the experiments on GUVs studying CTxB binding to unlabeled GM1, 1 mol% unlabeled GM1 (Avanti Polar Lipids) was added to the above DOPC/BSM/Chol mixture before GUV preparation.

2.3. GPMV preparation

In most experiments we prepared GPMVs from RBL-2H3 cells. For the control experiments of the CTxB-GM1 binding, GPMVs were isolated from CHO-K1 cells (which lack native GM1). We followed a procedure described in detail previously [64,65,86]. Briefly, after growing the cells to a confluence of 70–80%, GPMVs were isolated by chemically inducing cell blebbing with 25 mM paraformaldehyde (PFA) and 2 mM dithiothreitol (DTT) or 2 mM N-Ethylmaleimide (NEM) in a buffer (150 mM NaCl, 10 mM Hepes, 2 mM CaCl2, pH 7.4) for 1 h at 37 °C as previously described [15]. We added 0.1–1 μM of the labeled lipids and similar amounts of the Ld marking dyes DiO, DiI or DiD after GPMV isolation. Imaging of GPMVs was performed at 10 °C with a temperature controlled microscope stage (Bioptechs, PA, USA).

2.4. Confocal microscopy

GUVs and GPMVs were placed into BSA-coated Labtek chambers and imaged with a ConfoCor 2 scanning confocal microscope. 488 nm, 543 nm and 633 nm lasers were used for excitation of green (NBD, DiO, TF and BD-FL), orange (DiI, BD-TMR, Atto532 and Alexa555) and red fluorophores (DiD, Alexa647, Atto647N and KK114), respectively. BP 530–550, BP 585–615 and LP 650 filters were used in the multi-track mode to filter the respective fluorescence and record simultaneous images of up to three different colors.

2.5. Determination of Lo partitioning and lipid analog brightness

We determined the fraction of lipid analogs partitioning into the Lo phase from intensity line profiles of confocal images (Fig. 1A and Supplementary Fig. 2) using ImageJ-Line profile, as described [66]. The fluorescence intensities of the Lo and Ld phase, F_{Lo} and F_{Ld} respectively, were determined from the peaks of the line scan, where the different phases were identified by the Ld phase markers Fast DiO, Fast DiI or DiD. Opposite sides experienced the same polarization of the exciting lasers and were thus chosen to eliminate any bias in fluorescence intensity due to differences in laser excitation efficiency. The background values obtained from the pixels outside the vesicles were subtracted from peak values.

The Lo-partitioning coefficient (%Lo) is then (Supplementary Fig. 2):

$$\%Lo = \frac{F_{Lo}}{F_{Lo} + F_{Ld}}. \tag{1}$$

This relationship would not hold if the molecular brightness (cpp, counts per particle) of a given analog was dependent on the membrane environment, i.e. if the fluorescent yield was different in the two phases. For all the lipid analogs tested, we performed FCS in pure Lo (DOPC/BSM/Chol (10:50:40)) and pure Ld (DOPC/BSM/Chol (80:10:10)) GUVs to measure the brightness of analogs in each phase (cpp_{Lo} and cpp_{Ld}) (Supplementary Fig. 3). These compositions are representative of the coexisting phases in the DOPC/BSM/Chol (2:2:1) GUVs used for the partitioning experiments and were estimated using published phase diagrams and tie lines [67]. FCS experiments were carried out as described previously [68]. Briefly, the focal spot was placed either on the top or bottom of the GUVs with the optical settings kept the same for Lo and Ld vesicle measurements. Brightness values were obtained by fitting the autocorrelation curves with a two-dimensional one-component diffusion model:

$$G(\tau) = \frac{1}{N}\left(1 + \frac{\tau}{\tau_D}\right)^{-1}. \tag{2}$$

Normalized Lo partitioning values ($(Lo\%)_n$) were then calculated accounting for the relative brightness of the lipid analogs in two phases (Table 1):

$$(Lo\%)_n = \frac{(Lo\%)*(cpp_{Ld}/cpp_{Lo})}{(Lo\%)*(cpp_{Ld}/cpp_{Lo}) + (100-Lo\%)}. \tag{3}$$

2.6. C-Laurdan Generalized Polarization Analysis

Generalized polarization (GP) analysis of C-Laurdan fluorescence was performed to measure the difference in relative lipid packing/order in two model systems, GUVs and GPMVs. We added 4 μM of C-Laurdan directly to the vesicle suspensions after preparation of GUVs and GPMVs. C-Laurdan images were taken using a Bio-Rad two-photon setup with a Mira 2000 two-photon laser. Fluorescence of C-Laurdan was excited at 800 nm and the emission was collected using 425/50 and 525/70 filters in the ordered and disordered channels, respectively. A λ/4 plate was used to eliminate the photoselection property of C-Laurdan. The GP values were calculated as described previously [69].

2.7. STED-FCS measurements

STED-FCS data were recorded on a microscope outlined previously in detail [40,59,70]. Briefly, pulsed diode lasers at 633 nm (≈80 ps pulse width, LDH-P-635, PicoQuant, Berlin, Germany) or at 532 nm (≈80 ps pulse width, Pico-TA 532, PicoQuant) were used for

excitation of Atto647N or KK114 and Atto532 fluorescence, respectively, and the STED beams were provided by a Titanium:Sapphire laser system (MaiTai, Spectra-Physics, Mountain View, CA, USA)
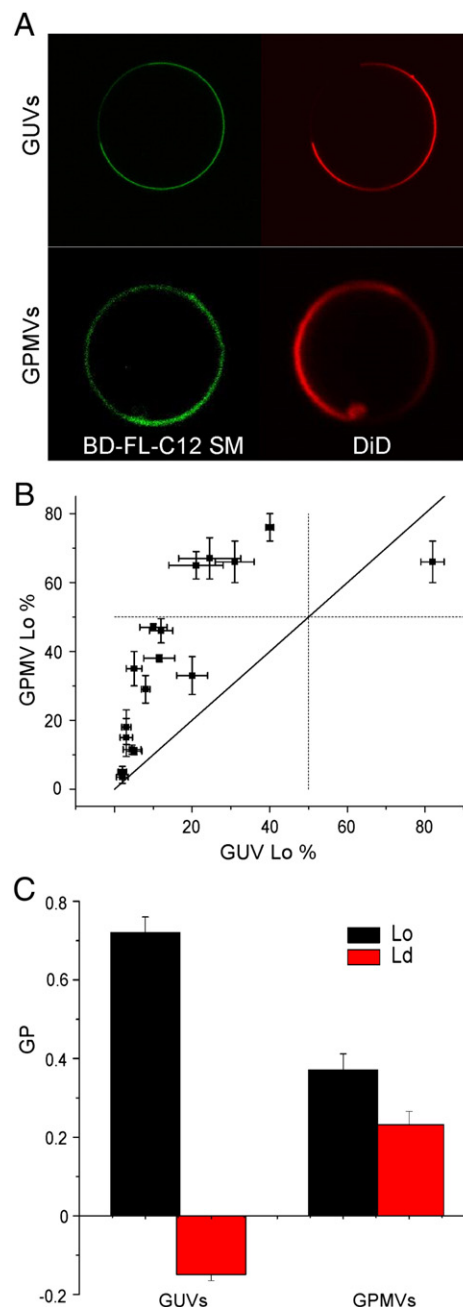
Fig. 1. Phase partitioning of fluorescent raft lipid analogs in GUVs and GPMVs. (A) Representative scanning confocal fluorescence images of phase separated GUVs and GPMVs stained with BD-FL-C12 SM and the Ld-phase marker DiD. The distribution of both molecules is revealed by the respective fluorescence intensities (green: BD-FL-C12 SM, red: DiD) and the %Lo values determined from the intensity ratios along the line profiles as shown in Figure S2. BD-FL-C12 SM prefers the Ld phase in GUVs (%Lo ≈ 30%) and the Lo phase in GPMVs (%Lo ≈ 65%). (B) Correlative plot of %Lo determined for the 18 different raft lipid analogs in GUVs and GPMVs. Most analogs prefer the Ld phase (%Lo < 50%, dashed lines) in GUVs; this mis-partitioning is less pronounced in GPMVs. (C) GP values of Ld (red columns) and Lo (black columns) domains in GUVs and GPMVs quantified by C-Laurdan microscopy. Larger GP values are indicative of higher molecular packing/order. Absolute ordering and the difference in order between phases is much more pronounced in GUVs than in GPMVs. Error bars represent standard deviations of the respective values determined from >10 vesicles/sample.

Table 1
Lo-partitioning of labeled SM, GM1 and cholesterol analogs in GUVs and GPMVs normalized for difference in fluorescence yield in the two phases (Eq. (3) and Fig. S3).

Lipid analog	GUV Lo%	GUV (Lo%)$_n$	GPMV Lo%
TF SM (AC)	20 ± 4	21 ± 4	33 ± 6
TF Chol (AC)	82 ± 3	80 ± 3	66 ± 6
BD-TMR Chol (AC)	40 ± 1	41 ± 1	76 ± 4
BD-FL-C5 SM (AC)	22 ± 4	25 ± 4	–
BD-FL-C12 SM (AC)	31 ± 5	31 ± 5	66 ± 6
BD-FL-C5 GM1 (AC)	21 ± 7	25 ± 7	65 ± 4
NBD-C12 SM (AC)	5 ± 2	5 ± 2	35 ± 5
NBD-C6 SM (AC)	12 ± 3	13 ± 3	46 ± 4
NBD-C6 GM1 (AC)	25 ± 8	23 ± 8	67 ± 6
Atto532 SM (AC)	10 ± 3	15 ± 3	47 ± 1
Atto532 SM (H)	12 ± 4	16 ± 4	38 ± 2
Atto647N SM (AC)	3 ± 1	4 ± 1	18 ± 5
Atto647N SM (H)	3 ± 1	3 ± 1	15 ± 6
Atto647N GM1 (AC)	5 ± 2	6 ± 2	11 ± 1
Atto647N GM1 (H)	8 ± 1	8 ± 1	26 ± 4
Atto647N SM Lyso (H)	2 ± 1	3 ± 1	5 ± 2
KK114 SM (AC)	2 ± 1	2 ± 1	4 ± 2
KK114 SM (H)	5 ± 2	5 ± 2	12 ± 1

operating at 770–780 nm with a repetition rate of 76 MHz, either directly for Atto647N or KK114 and at 612 nm for Atto532 by an optical parametric oscillator (APE, Berlin, Germany) fed by the same Titanium:Sapphire laser system. Fluorescence excitation and collection was realized using an oil immersion objective (PLAPON 60×, $NA = 1.42$, Olympus, Japan; or HCXPLAPO $NA = 1.4$, Leica Microsystems). The 50:50 split fluorescence signal was detected by two single-photon counting modules (avalanche photo diode SPCM-AQR-13-FC, Perkin Elmer Optoelectronics, Fremont, CA, USA) and the recorded fluorescence counts were further processed by a hardware correlator card (Flex02-01D, Correlator.com, NJ, USA).

Mammalian PtK2 cells were prepared, and incorporation of the lipids into the plasma membrane via a BSA–lipid complex was performed as previously described [40,70].

STED-FCS measurements were performed at room temperature by placing the foci on random positions in the lower plasma membrane facing the coverslip, and by completing all measurements before significant internalization or any morphological changes in the cell could take place. The measurement times were kept short (~15 s) to avoid biasing distortion of the correlation data due to very infrequent transits of bright particles such as cell debris [40,70].

Fitting of the FCS data was performed by using a two-dimensional diffusion model assuming a Gaussian-shaped fluorescence detection profile [40,70].

$$G(t_c) = 1 + (1/N)\left(1 + (t_c/\tau_D)^\alpha\right)^{-1}. \tag{4}$$

Here, $\tau_D = d^2/(8 \ln2\, D)$ denotes the average transit time through the focal spot of diameter (or full-width-at-half-maximum) d, D the apparent diffusion coefficient and α the anomaly coefficient, which is $=1$ for normal free Brownian diffusion and <1 for heterogeneous diffusion, for example, due to trapping. Additional terms due to dark (triplet) state populations were regarded as detailed in [40,70].

3. Results and discussion

3.1. Partitioning in GUVs

GUVs composed of DOPC/BSM/Chol (2:2:1) displayed separation into an Ld and an Lo phase at room temperature, revealed by a heterogeneous distribution of the dyes Fast DiO, Fast DiI or DiD-C18 (Fig. 1A). All of these dyes are known to incorporate into the membrane and specifically mark the Ld phase [16]. This domain assignment was confirmed by Generalized Polarization (GP) experiments

using the membrane marker C-Laurdan: the Lo phase is characterized by relatively high GP values, compared to the Ld phase [8] (Fig. 1C). We determined the Lo partitioning (%Lo; Eq. (3)) of various fluorescent analogs of sphingomyelin (SM), GM1 and cholesterol (Chol), which were either labeled with the dye NBD, TopFluor (TF), Bodipy-FL (BD-FL), Bodipy-TMR (BD-TMR), Atto532, Atto647N or KK114, from intensity line profiles of scanning confocal fluorescence images (Fig. 1A, Supplementary Fig. 2). The fluorescent raft lipid analogs were either labeled on the headgroup (H) or by replacement of the native acyl chain with a short acyl chain carrying the dye (AC) (for structures see Supplementary Fig. 1). Non-labeled SM, GM1, and cholesterol would be predicted to enrich in the Lo phase based on their preference for raft domains in live cells, as assayed by detergent resistance [71,72]. The orientation of the tie lines in tertiary mixtures confirms this assumption for SM, and to a much smaller extent, cholesterol [11]. Lo enrichment of GM1 is predicted by binding of its ligand cholera toxin [72]. Based on this information, deviation from Lo preference for SM, GM1, and cholesterol analogs can be attributed to the influence of the label.
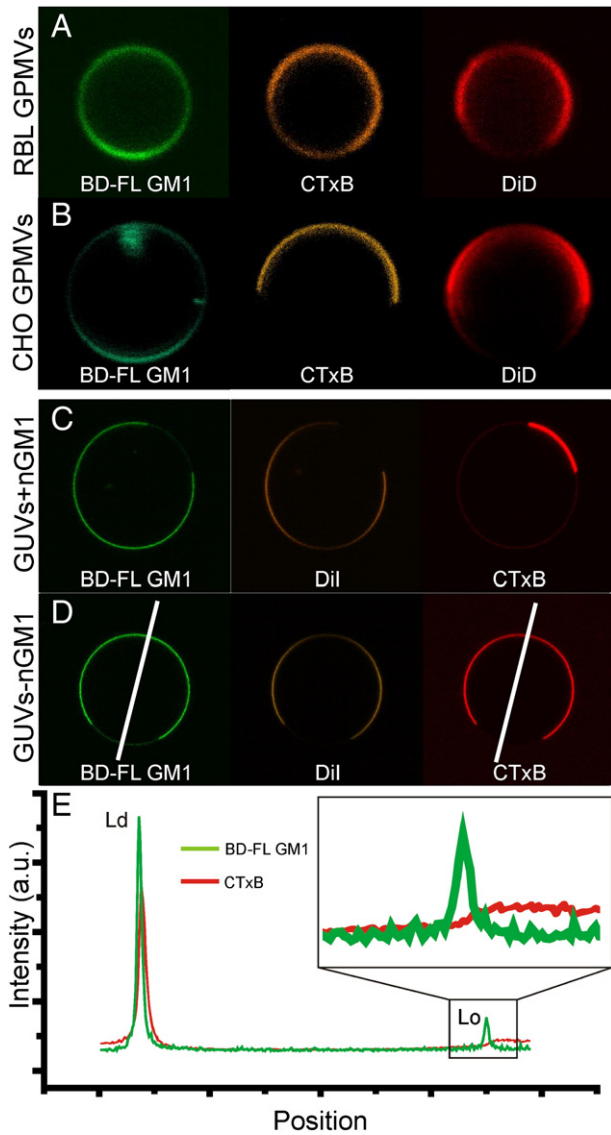
Fig. 1A (upper panel) shows representative fluorescence scanning images of a GUV incorporating the dye DiD and a SM analog (BD-FL C12 SM). This analog preferentially partitions into the phase marked by DiD, i.e. the Ld phase. Using the procedure described in Eq. (3), we determined %Lo ≈ 30%. Table 1 lists the %Lo values for all fluorescent raft analogs tested here. 17 of the 18 analogs tested (TF-Chol excepted) were enriched in the disordered phase (%Lo < 50%) in GUVs, in agreement with previous observations for other lipid analogs [36–38,44,45,50,52,53,73]. The mis-partitioning of raft analogs labeled by acyl chain replacement is expected, because the addition of the bulky fluorescent side-chain may change the packing abilities of the lipid. In the case of headgroup labeling, mis-partitioning may be explained by a label-induced change of the headgroup conformation and/or by the dye label tilting towards the membrane, again introducing a steric hindrance.

3.2. Differential partitioning of lipid analogs in GUVs and GPMVs

GPMVs derived from RBL cells showed phase separation similar to that of GUVs (Fig. 1A bottom). However, nearly all analogs were much more ordered phase preferring in GPMVs (%Lo (GPMV) > %Lo (GUV), Fig. 1B) regardless of the chemical preparation used to derive the vesicles (i.e. PFA/DTT or NEM; all data shown is from PFA/DTT GPMVs). This model system-dependent partitioning is likely due to the difference in order/packing of the lipids in the coexisting phases of the GUVs compared to GPMVs [74–76]. Similar to previous reports [77], we used C-Laurdan microscopy to measure the molecular packing (and thus order) of the Ld and Lo phases in the vesicles (Fig. 1C). In the DOPC/BSM/Chol GUVs, the Ld phase was much more disordered, and the Lo phase much more ordered, than in the GPMVs. Consequently, the order difference between the coexisting phases was much larger for these GUVs than for the GPMVs (as observed in previous experiments [77]), likely amplifying the inherent disorder preference of many lipid analogs in the case of the GUVs. The quite small order difference between domains in GPMVs is presumably due to their complex lipid and protein content, likely resulting in a more biologically appropriate molecular partitioning than modeled in GUVs.

3.3. Label size, hydrophobicity, and position affect analog partitioning
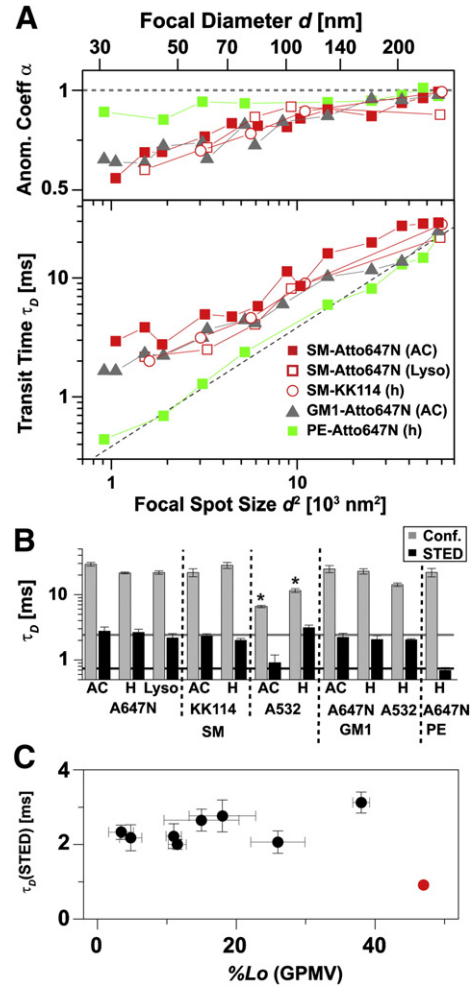
Having determined that GPMVs provide a more physiological system to measure lipid analog partitioning between coexisting liquid phases, we attempted to determine the dependence of this partitioning on specific structural factors such as label type, label position, and lipid headgroup. Lo partitioning of SM was in general lowest for the most bulky and charged dye labels Atto647N, KK114 and Atto532 (%Lo values down to <2% and <4% in GUVs and GPMVs, respectively

and zwitterionic analogs (TF and BD-FL). This effect may be attributed to the hydrophilic nature of NBD, which is evidenced by the relatively poor integration of NBD-labeled lipids into membranes [40]. Further, NBD-labeled lipid analogs have been shown to partition to the hydrophobic/hydrophilic interface of the membrane [79], thereby disrupting the local packing of the membrane. However, this effect cannot be generalized since NBD-labeled GM1 prefers the ordered phase (Table 1). Moreover, hydrophobicity of the dye does not completely determine Lo preference: the most hydrophobic label of all (Atto647N) drives SM into the disordered phase, while the same lipid labeled with the

Fig. 2. Phase specific binding of GM1 to CTxB. Representative scanning confocal fluorescence images of phase separated GPMVs (A,B) and GUVs (C,D) stained with BD-FL-C5 GM1 (green), Alexa555 labeled CTxB (orange) and the disorder marker DiD (red) along with (E) intensity profile along the lines marked in (D) for BD-FL-C5 and CTxB. In GPMVs (A,B), the labeled GM1 enriches in Lo phase (%Lo ≈ 65%). In RBL-derived GPMVs (A), which contain native GM1, CTxB binds both phases, while in CHO-derived GPMVs (B), which lack native GM1, CTxB binds exclusively to the Ld phase. In GUVs containing both labeled and native GM1 (C, GUVs + nGM1), CTxB is highly enriched in the Lo phase (presumably containing the native GM1) with some Ld binding (presumably to the labeled GM1, intensity line profile in E). In GUVs lacking native GM1 and having only BD-FL-C5 GM1 (D, GUVs-nGM1), CTxB exclusively binds to the Ld domain. Thus, while CTxB binds unlabeled GM1 in the Lo phase, it binds labeled GM1 only in the Ld phase.

— Atto647N is positively charged and KK114 and Atto532 have a negative net charge) and highest for the smaller and uncharged dye labels NBD, TF and BD-FL (%Lo up to 65% in GPMVs; TF and BD-FL are zwitterionic with a very small charge separation). Therefore, it seems that it is advantageous to use smaller and uncharged dye labels. In agreement with this conclusion, a lipid labeled with an uncharged NileRed derivative has previously been shown to be Lo preferring [78] (this derivative did not represent a functional lipid, such as a sphingolipid). Label steric size and charge are not the only determinants of partitioning, since SM labeled with the smallest and completely uncharged moiety NBD was less Lo preferring (%Lo < 50% in GPMVs) than slightly larger

Fig. 3. STED-FCS measurements of fluorescent raft lipid analogs in the plasma membrane of living cells and comparison to phase partitioning. (A) Anomaly coefficient α and average transit time τ_D for different fluorescent SM and GM1 lipids and for a fluorescent PE lipid determined by fitting Eq. (4) to the FCS data recorded for different focal spots tuned by STED. An anomaly coefficient $\alpha \approx 1$ and a linear dependence of τ_D on the focal spot size (proportional diameter-squared d^2) indicated free diffusion (dotted line, diffusion coefficient $D = 0.45 \, \mu m^2/s$), while $\alpha < 1$ and a deviation of τ_D towards larger values for small focal spots indicated transient trapping events. (B) Average transit time τ_D of different fluorescent SM, GM1 and PE lipid analogs for confocal ($d \approx 240$ nm or ≈ 180 nm (star), gray columns) and STED recordings ($d \approx 40$ nm, black columns). The SM and GM1 analogs showed increased transit times τ_D for the STED recordings indicating trapping (gray line) while a PE analog and the SM analog labeled at the acyl chain with the very hydrophilic dye Atto532 (532 AC) showed a low τ_D in accordance with almost free diffusion (black line). The confocal recordings failed to report this difference. Values and error bars represent the average and the standard deviation of the mean from at least 30 measurements on different spots of different cells (A = Atto). (C) Nanoscale trapping as probed by STED-FCS and phase partitioning are uncorrelated: comparison of transit times τ_D (STED-FCS, $d \approx 40$ nm) and Lo partitioning coefficient %Lo in GPMVs (Table 1) for the lipids presented in B (red dot: Atto532 SM (AC)).

similarly bulky but very hydrophilic dye Atto532 (shown to be hardly membrane anchored [40]) was much more Lo preferring (%Lo in GPMVs nearly 50%).

Using the Atto647N, KK114 and Atto532 labeled SM and GM1 derivatives, we studied the influence of the dye position (acyl chain replacement versus headgroup attachment (H)) on the phase affiliation. The position had no observable influence for Atto532- and Atto647N SM (even when comparing it to the headgroup labeled Lyso derivative): Lo partitioning was always low. However, headgroup-labeling slightly improved the Lo affinity for Atto647N-GM1 and KK114 SM.

Finally, we evaluated the effect of labeling at different positions on the acyl chain by comparing SM labeled with BD-FL and NBD at the end of a short versus a long acyl tail (C5 or C6 versus C12). In GUVs, the longer acyl chain (C12) derivative was slightly more Lo preferring for BD-FL but less for NBD. In GPMVs, C6 versus C12 had no significant effect on NBD (%Lo ≈ 46% compared to 35%) but we observed a surprising behavior for the BD-FL SM analogs (Supplementary Fig. 4): in contrast to the C12 derivative with a %Lo > 60%, the BD-FL-C5 analog penetrated through the GPMV membrane and accumulated inside the vesicles.

We conclude that partitioning of a lipid analog is a complex combination of a multitude of factors, such as the polarity, size and charge of the label, the label position and headgroup size of the lipid, that influence the ability of the analog to be inserted into the more restrictive ordered phase. However, it seems that the use of small and uncharged dye tags is more likely to preserve ordered phase partitioning.

3.4. Labeling affects binding of GM1 to CTxB

The B subunit of cholera toxin (CTxB) is known to specifically bind to GM1, preferably in the ordered phase [17]. We therefore investigated how the mis-partitioning of fluorescently labeled GM1 influences its binding to CTxB. We labeled GPMVs derived from RBL cells with DiD (as a reference for the disordered phase) and GM1 with BD-FL at the end of a C5 acyl chain linker (BD-FL-C5 GM1 (AC)), then added Alexa555-labeled CTxB to determine the phase preference of the labeled CTxB from the simultaneously recorded multicolor confocal scanning images (Fig. 2). BD-FL-C5 GM1 has a slight preference for the Lo phase (%Lo ≈ 65%, Fig. 1 and Table 1). CTxB binding to GM1 was observed in both phases, with an unexpected enrichment in the disordered phase (Fig. 2A); however, it was impossible to make a clear assignment for the binding to the labeled GM1, since the GPMVs derived from RBL cells contained native GM1 in addition to the exogenous GM1 analog.

To isolate the effect of labeled GM1 from native GM1, we measured CTxB binding to GPMVs isolated from a Chinese Hamster Ovary subtype (CHO-K1) that does not produce complex gangliosides [65]. In the absence of exogenous GM1, CTxB did not bind to these vesicles, consistent with their lack of native GM1 (data not shown). When labeled GM1 was added to these CHO-K1 derived GPMVs, we observed partitioning of BD-FL-C5 GM1 similar to RBL GPMVs (%Lo ≈ 66%). However, while there was still weak binding of CTxB to Lo phase in RBL GPMVs presumably due to the native GM1, we observed a very selective binding of CTxB to the Ld phase and no Lo binding in CHO GPMVs (Fig. 2B). Thus, since labeled GM1 is present in both phases while CTxB signal is only observed in the Ld phase, CTxB can only bind the Ld, but not the Lo pool of BD-FL-C5 GM1. All of these results were the same when using Alexa647 instead of Alexa555 as a label for CTxB.

To confirm this conclusion in a controlled system, we produced GUVs containing only labeled GM1, or both labeled and unlabeled GM1, and determined the phase preference of CTxB binding (Fig. 2C–E). In GUVs (with or without native GM1), the labeled GM1 mainly partitioned into the Ld phase with ~20% of the molecules entering the Lo phase. In presence of native GM1, CTxB bound highly preferentially to the Lo domain (Fig. 2C), consistent with partitioning of its native ganglioside receptor to the ordered phase. When only labeled GM1 was included in the GUVs, CTxB bound exclusively to the Ld domain (Fig. 2D and red line in 2E), despite the presence of BD-FL-C5 GM1 in the ordered phase (Fig. 2D and green line in 2E).

Thus, the addition of the fluorescent dye label to the ganglioside GM1 acyl chain not only affects the phase partitioning of the lipid, but also impairs the binding of ligand to its head group. We speculate that for the labeled GM1, the conformation of the polar headgroup is different in the Lo than in the Ld phase. The headgroup may be tilted in the Lo phase [80,81], accounting for the perturbed binding. CTxB cooperatively binds up five GM1 lipids and this multivalency may be disturbed in case of the altered conformation. Most importantly, this effect demonstrates that bulk membrane properties (in this case, the ordering or molecular packing) have an effect on the interaction of a ligand with its membrane-bound lipid receptor in biologically-complex environments.

3.5. Partitioning of lipid analogs is uncorrelated with their nanoscale diffusion in living cells

Several novel imaging methods have recently been developed to probe live cells at spatial resolutions well below the limit imposed by diffraction. These methods can reveal nanometer-scale structures on the order of the proposed spatiotemporal scales of lipid rafts. We used the combination of STED nanoscopy [56–58] and FCS, STED-FCS [40,70], to determine the affinity of several of the previously mentioned fluorescent lipid analogs to transient nanoscale complexes previously observed in the plasma membrane of living cells [40,59]. A great advantage of the STED method is the ability to continuously tune the size of the effective focal spot through which lipid molecules may diffuse, from diffraction-limited $d = 240$ nm (or 180 nm depending on the excitation wavelength) down to molecular scales, and to determine their average transit times τ_D using FCS, as shown in Fig. 3A. While freely diffusing molecules show a linear dependence of the focal transit time τ_D on the focal area ($\sim d^2$), transient trapping leads to relatively increased values of τ_D for smaller focal spots [82]. This is because the focal spot size becomes adequately small to ensure that the time of trapping sufficiently exceeds the focal dwelling time of free diffusion [40]. As a consequence, the description of the FCS data of such heterogeneous diffusion has to include an anomaly coefficient $\alpha < 1$ (Eq. (4)). Fig. 3A depicts exemplary STED-FCS data of several fluorescent SM and GM1 lipid analogs, which all congruently showed the mentioned characteristic behavior for transient trapping, while an Atto647N labeled phosphoethanolamine (PE) exhibited the characteristic linear dependence of τ_D on d^2 and $\alpha \approx 1$ of close to free diffusion. Screening of several differently labeled SM and GM1 molecules showed no dependence of their dynamical and trapping characteristics on the dye and its position (Fig. 3B), indicating a negligible influence of the dye. We only investigated the lipid analogs labeled with Atto647N, KK114 and Atto532 with STED-FCS, because the absorption and emission spectrum of these dyes were the only ones that suited the present STED-FCS setups.

All SM and GM1 analogs used for STED-FCS were Ld-preferring in both GUVs and GPMVs with a significant variety in quantitative partitioning values (Table 1, %Lo of 2–50%). This variable partitioning was in striking contrast to the parity of diffusion behavior observed for the very same dyes with STED-FCS (Fig. 3B). Indeed, no quantitative correlation between these two parameters could be discerned (Fig. 3C). Most strikingly, SM labeled at the acyl chain with the very hydrophilic dye Atto532 (Atto532 SM (AC)) showed the largest Lo affinity of all lipid analogs investigated by STED-FCS (%Lo(GPMV) = 47%), but its diffusion characteristics was strongly biased in the plasma membrane of intact living cells: diffusion of Atto532 SM (AC) was much faster than for the other SM analogs and trapping was almost abolished, probably due to its high polarity and the resulting weak membrane

anchoring of the analog [40] (Fig. 3B,C). These results suggest a different physical nature for the nanoscale trapping observed in intact living cells using STED-FCS and phase partitioning in isolated phase-separated plasma membrane.

4. Conclusion

To better understand the behavior of widely used fluorescent lipid analogs [49,53], this study systematically investigates the partitioning of a multitude of fluorescent cholesterol, SM and GM1 analogs in two different model systems (fully synthetic GUVs and cell-derived GPMVs), and relates it to their nanoscale dynamics in intact cellular plasma membranes. Our results reveal the following:

(i) In agreement with several previous observations [16,43,46, 49–53], most fluorescently labeled analogs of raft lipids do not partition into ordered phases, in contrast to their native counterparts.

(ii) The partitioning of a lipid analog is a complex function of type, size, polarity, charge and position of the dye tag, with a tendency of smaller and uncharged dye tags more likely to preserve ordered phase partitioning.

(iii) Labeling may not only affect the phase preference of a lipid, but also directly modulate its biological activity in a phase-specific manner, as shown for the CTxB-GM1 interaction. While CTxB preferably binds unlabeled GM1 in the Lo phase, the binding affinity between acyl-chain labeled GM1 and CTxB is higher in the Ld phase.

(iv) Mis-partitioning of raft lipid analogs is much less pronounced in cell-derived GPMVs than in DOPC/BSM/Chol GUVs, suggesting that GPMVs are more appropriate models for biological systems. In spite of their value for studying membrane phase separation in general, commonly used DOPC/SM/Chol GUVs appear to be rather problematic models to mimic the cell membrane heterogeneity, not only because of their limited complexity, but also due to the seemingly quite different physical nature of the domains.

(v) Nanoscale diffusion and trapping of fluorescent raft lipids in the plasma membrane of intact living cells as observed by STED-FCS and phase partitioning in model membranes are uncorrelated, i.e. STED-FCS may be probing a property of the membrane that is not related to phase separation in GUVs and GPMVs.

It is important to point out that both model membrane systems are likely in a state of thermodynamic equilibrium, while the plasma membrane of living cells is dynamic and non-equilibrated. Interactions in a dynamic and un-equilibrated system such as the plasma membrane of intact living cells may be destroyed in GPMVs by the absence of some important cellular structures, such as the cytoskeleton and/or by equilibrating the system as, for example, done by reducing the temperature [83–85]. As a consequence, as already discussed for the difference between GUVs and GPMVs, the difference in order (or other physical properties) between lipid domains in living, non-equilibrated cellular membranes may be smaller than of any currently available model system. It is important to stress that although phase coexistence in lipid model systems is often viewed as an analog of raft behavior in the cell membrane, it may not necessarily be accurate to assign the "native behavior" of a lipid analog based on its partitioning in these systems. As we have shown, probe geometry and chemistry are important factors for the partitioning behavior of lipid analogs, while their confined diffusion in intact living cells indicates that the chemistry behind the confining interactions is unaffected by labeling. Most likely, in intact living cells, STED-FCS has probed the formation of transient, chemically specific interactions between raft lipids and other membrane constituents (such as other lipids and proteins) that may comprise the physicochemical basis of lipid–protein platforms. Lo-preferring fluorescent raft analogs

are then used observe the coalesced (i.e. large, long-lived, equilibrium domains) state of these platforms.

Supplementary materials related to this article can be found online at doi:10.1016/j.bbamem.2012.03.007.

References

[1] P. Schwille, S. Diez, Synthetic biology of minimal systems, Crit. Rev. Biochem. Mol. Biol. 44 (2009) 223–242.
[2] M. Loose, P. Schwille, Biomimetic membrane systems to study cellular organization, J. Struct. Biol. 168 (2009) 143–151.
[3] M.I. Angelova, D.S. Dimitrov, Liposome electroformation, Faraday Discuss. 81 (1986) 303.
[4] M.I. Angelova, D.S. Dimitrov, A mechanism of liposome electroformation, Prog. Colloid Polym. Sci. 76 (1988) 59–67.
[5] M.I. Angelova, S. Soléau, P. Méléard, F. Faucon, P. Bothorel, Preparation of giant vesicles by external AC electric fields. Kinetics and applications, Prog. Colloid Polym. Sci. 89 (1992) 127–131.
[6] K. Bacia, D. Scherfeld, N. Kahya, P. Schwille, Fluorescence correlation spectroscopy relates rafts in model and native membranes, Biophys. J. 87 (2004) 1034–1043.
[7] K. Bacia, P. Schwille, T. Kurzchalia, Sterol structure determines the separation of phases and the curvature of the liquid-ordered phase in model membranes, Proc. Natl. Acad. Sci. U. S. A. 102 (2005) 3272–3277.
[8] C. Dietrich, L.A. Bagatolli, Z.N. Volovyk, N.L. Thompson, M. Levi, K. Jacobson, E. Gratton, Lipid rafts reconstituted in model membranes, Biophys. J. 80 (2001) 1417–1428.
[9] N. Kahya, D. Scherfeld, K. Bacia, B. Poolman, P. Schwille, Probing lipid mobility of raft-exhibiting model membranes by fluorescence correlation spectroscopy, J. Biol. Chem. 278 (2003) 28109–28115.
[10] N. Kahya, D. Scherfeld, K. Bacia, P. Schwille, Lipid domain formation and dynamics in giant unilamellar vesicles explored by fluorescence correlation spectroscopy, J. Struct. Biol. 147 (2004) 77–89.
[11] S.L. Veatch, S.L. Keller, Organization in lipid membranes containing cholesterol, Phys. Rev. Lett. 89 (2002).
[12] S.L. Veatch, S.L. Keller, Separation of liquid phases in giant vesicles of ternary mixtures of phospholipids and cholesterol, Biophys. J. 85 (2003) 3074–3083.
[13] R.E. Scott, Plasma membrane vesiculation: a new technique for isolation of plasma membranes, Science 194 (1976) 743–745.
[14] R.E. Scott, P.B. Maercklein, L.T. Furcht, Plasma membrane intramembranous particle topography in 3T3 and SV3T3 cells: the effect of cytochalasin B, J. Cell Sci. 23 (1977) 173–192.
[15] T. Baumgart, A.T. Hammond, P. Sengupta, S.T. Hess, D.A. Holowka, B.A. Baird, W.W. Webb, Large-scale fluid/fluid phase separation of proteins and lipids in giant plasma membrane vesicles, Proc. Natl. Acad. Sci. U. S. A. 104 (2007) 3165–3170.
[16] T. Baumgart, G. Hunt, E.R. Farkas, W.W. Webb, G.W. Feigenson, Fluorescence probe partitioning between L-o/L-d phases in lipid membranes, Biochim. Biophys. Acta, Biomembr. 1768 (2007) 2182–2194.
[17] I. Leventan, F.J. Byfield, P. Chowdhury, F. Gai, T. Baumgart, P.A. Janmey, Cholesterol-dependent phase separation in cell-derived giant plasma-membrane vesicles, Biochem. J. 424 (2009) 163–167.
[18] H. Keller, M. Lorizate, P. Schwille, PI(4,5)P-2 degradation promotes the formation of cytoskeleton-free model membrane systems, Chemphyschem 10 (2009) 2805–2812.
[19] S.L. Veatch, P. Cicuta, P. Sengupta, A. Honerkamp-Smith, D. Holowka, B. Baird, Critical fluctuations in plasma membrane vesicles, ACS Chem. Biol. 3 (2008) 287–293.
[20] J. Nikolaus, S. Scolari, E. Bayraktarov, N. Jungnick, S. Engel, A.P. Plazzo, M. Stockl, R. Volkmer, M. Veit, A. Herrmann, Hemagglutinin of influenza virus partitions into the nonraft domain of model membranes, Biophys. J. 99 (2010) 489–498.
[21] K. Bacia, C.G. Schuette, N. Kahya, R. Jahn, P. Schwille, SNAREs prefer liquid-disordered over "raft" (liquid-ordered) domains when reconstituted into giant unilamellar vesicles, J. Biol. Chem. 279 (2004) 37951–37955.
[22] K. Simons, E. Ikonen, Functional rafts in cell membranes, Nature 387 (1997) 569–572.
[23] U. Coskun, K. Simons, Membrane rafting: from apical sorting to phase segregation, FEBS Lett. 584 (2010) 1685–1693.
[24] S. Engel, S. Scolari, B. Thaa, N. Krebs, T. Korte, A. Herrmann, M. Veit, FLIM-FRET and FRAP reveal association of influenza virus haemagglutinin with membrane rafts, Biochem. J. 425 (2010) 567–573.
[25] S. Mayor, M. Rao, Rafts: scale-dependent, active lipid organization at the cell surface, Traffic 5 (2004) 231–240.
[26] S. Mayor, H. Riezman, Sorting GPI-anchored proteins, Nat. Rev. Mol. Cell Biol. 5 (2004) 110–120.

[27] M. Rao, S. Mayor, Use of Forster's resonance energy transfer microscopy to study lipid rafts, Biochim. Biophys. Acta, Mol. Cell. Res. 1746 (2005) 221–233.

[28] F. Pinaud, X. Michalet, G. Iyer, E. Margeat, H.P. Moore, S. Weiss, Dynamic partitioning of a glycosyl-phosphatidylinositol-anchored protein in glycosphingolipid-rich microdomains imaged by single-quantum dot tracking, Traffic 10 (2009) 691–712.

[29] C. Depry, M.D. Allen, J. Zhang, Visualization of PKA activity in plasma membrane microdomains, Mol. Biosyst. 7 (2011) 52–58.

[30] A.M. Navratil, S.P. Bliss, M.S. Roberson, Membrane rafts and GnRH receptor signaling, Brain Res. 1364 (2010) 53–61.

[31] A.H. Pillet, V. Lavergne, V. Pasquier, F. Gesbert, T. Theze, T. Rose, IL-2 induces conformational changes in its preassembled receptor core, which then migrates in lipid raft and binds to the cytoskeleton meshwork, J. Mol. Biol. 403 (2010) 671–692.

[32] K. Simons, M.J. Gerl, Revitalizing membrane rafts: new tools and insights, Nat. Rev. Mol. Cell Biol. 11 (2010) 688–699.

[33] P. Sengupta, A. Hammond, D. Holowka, B. Baird, Structural determinants for partitioning of lipids and proteins between coexisting fluid phases in giant plasma membrane vesicles, Biochim. Biophys. Acta, Biomembr. 1778 (2008) 20–32.

[34] C. Schultz, A.B. Neef, T.W. Gadella Jr., J. Goedhart, Imaging lipids in living cells, Cold Spring Harb. Protoc. 7 (2010).

[35] L. Kuerschner, C.S. Ejsing, K. Ekroos, A. Shevchenko, K.I. Anderson, C. Thiele, Polyene-lipids: a new tool to image lipids, Nat. Methods 2 (2005) 39–45.

[36] I.A. Boldyrev, X.H. Zhai, M.M. Momsen, H.L. Brockman, R.E. Brown, J.G. Molotkovsky, New BODIPY lipid probes for fluorescence studies of membranes, J. Lipid Res. 48 (2007) 1518–1532.

[37] M. Holtta-Vuori, R.L. Uronen, J. Repakova, E. Salonen, I. Vattulainen, P. Panula, Z.G. Li, R. Bittman, E. Ikonen, BODIPY-cholesterol: a new tool to visualize sterol trafficking in living cells and organisms, Traffic 9 (2008) 1839–1849.

[38] D.L. Marks, R. Bittman, R.E. Pagano, Use of BODIPY-labeled sphingolipid and cholesterol analogs to examine membrane microdomains in cells, Histochem. Cell Biol. 130 (2008) 819–832.

[39] J. Oreopoulos, C.M. Yip, Probing membrane order and topography in supported lipid bilayers by combined polarized total internal reflection fluorescence-atomic force microscopy, Biophys. J. 96 (2009) 1970–1984.

[40] C. Eggeling, C. Ringemann, R. Medda, G. Schwarzmann, K. Sandhoff, S. Polyakova, V.N. Belov, B. Hein, C. von Middendorff, A. Schonle, S.W. Hell, Direct observation of the nanoscale dynamics of membrane lipids in a living cell, Nature 457 (2009) 1159–1162.

[41] D. Tyteca, L. D'Auria, P. Van Der Smissen, T. Medts, S. Carpentier, J.C. Monbaliu, P. de Diesbach, P.J. Courtoy, Three unrelated sphingomyelin analogs spontaneously cluster into plasma membrane micrometric domains, Biochim. Biophys. Acta, Biomembr. 1798 (2010) 909–927.

[42] N. Ichikawa, K. Iwabuchi, H. Kurihara, K. Ishii, T. Kobayashi, T. Sasaki, N. Hattori, Y. Mizuno, K. Hozumi, Y. Yamada, E. Arikawa-Hirasawa, Binding of laminin-1 to monosialoganglioside GM1 in lipid rafts is crucial for neurite outgrowth, J. Cell Sci. 122 (2009) 289–299.

[43] O. Coban, M. Burger, M. Laliberte, A. Ianoul, L.J. Johnston, Ganglioside partitioning and aggregation in phase-separated monolayers characterized by BODIPY GM1 monomer/dimer emission, Langmuir 23 (2007) 6704–6711.

[44] I. Mikhalyov, N. Gretskaya, L.B.A. Johansson, Fluorescent BODIPY-labelled G(M1) gangliosides designed for exploring lipid membrane properties and specific membrane–target interactions, Chem. Phys. Lipids 159 (2009) 38–44.

[45] S.M. Polyakova, V.N. Belov, S.F. Yan, C. Eggeling, C. Ringemann, G. Schwarzmann, A. de Meijere, S.W. Hell, New gm1 ganglioside derivatives for selective single and double labelling of the natural glycosphingolipid skeleton, Eur. J. Org. Chem. (2009) 5162–5177.

[46] J.E. Shaw, R.F. Epand, R.M. Epand, Z.G. Li, R. Bittman, C.M. Yip, Correlated fluorescence-atomic force microscopy of membrane domains: structure of fluorescence probes determines lipid localization, Biophys. J. 90 (2006) 2170–2178.

[47] C. Wan, V. Kiessling, L.K. Tamm, Coupling of cholesterol-rich lipid phases in asymmetric bilayers, Biochemistry 47 (2008) 2190–2198.

[48] A.R. Burns, D.J. Frankel, T. Buranda, Local mobility in lipid domains of supported bilayers characterized by atomic force microscopy and fluorescence correlation spectroscopy, Biophys. J. 89 (2005) 1081–1093.

[49] N. Kahya, Light on fluorescent lipids in rafts: a lesson from model membranes, Biochem. J. 430 (2010) e7–e9.

[50] O. Maier, V. Oberle, D. Hoekstra, Fluorescent lipid probes: some properties and applications (a review), Chem. Phys. Lipids 116 (2002) 3–18.

[51] D. Wustner, Fluorescent sterols as tools in membrane biophysics and cell biology, Chem. Phys. Lipids 146 (2007) 1–25.

[52] T.Y. Wang, J.R. Silvius, Different sphingolipids show differential partitioning into sphingolipid/cholesterol-rich domains in lipid bilayers, Biophys. J. 79 (2000) 1478–1489.

[53] J. Juhasz, J.H. Davis, F.J. Sharom, Fluorescent probe partitioning in giant unilamellar vesicles of 'lipid raft' mixtures, Biochem. J. 430 (2010) 415–423.

[54] A. Kusumi, H. Ike, C. Nakada, K. Murase, T. Fujiwara, Single-molecule tracking of membrane molecules: plasma membrane compartmentalization and dynamic assembly of raft-philic signaling molecules, Semin. Immunol. 17 (2005) 3–21.

[55] A. Kusumi, Y.M. Shirai, I. Koyama-Honda, K.G.N. Suzuki, T.K. Fujiwara, Hierarchical organization of the plasma membrane: investigations by single-molecule tracking vs. fluorescence correlation spectroscopy, FEBS Lett. 584 (2010) 1814–1823.

[56] S.W. Hell, Far-field optical nanoscopy, Science 316 (2007) 1153–1158.

[57] T.A. Klar, M. Dyba, S.W. Hell, Stimulated emission depletion microscopy with an offset depleting beam, Appl. Phys. Lett. 78 (2001) 393–395.

[58] S.W. Hell, J. Wichmann, Breaking the diffraction resolution limit by stimulated emission: stimulated-emission-depletion fluorescence microscopy, Opt. Lett. 19 (1994) 780–782.

[59] V. Mueller, C. Ringemann, A. Honigmann, G. Schwarzmann, R. Medda, M. Leutenegger, S. Polyakova, V.N. Belov, S.W. Hell, C. Eggeling, STED nanoscopy reveals molecular details of cholesterol- and cytoskeleton-modulated lipid interactions in living cells, Biophys. J. 101 (2011) 1651–1660.

[60] A. Honigmann, C. Walter, F. Erdmann, C. Eggeling, R. Wagner, Characterization of horizontal lipid bilayers as a model system to study lipid phase separation, Biophys. J. 98 (2010) 2886–2894.

[61] K. Kolmakov, V.N. Belov, J. Bierwagen, C. Ringemann, V. Muller, C. Eggeling, S.W. Hell, Red-emitting rhodamine dyes for fluorescence microscopy and nanoscopy, Chem. Eur. J. 16 (2010) 158–166.

[62] G. Schwarzmann, K. Sandhoff, Lysogangliosides: synthesis and use in preparing labeled gangliosides, Methods Enzymol. 138 (1987) 319–341.

[63] A.J. Garcia-Saez, D.C. Carrer, P. Schwille, Fluorescence correlation spectroscopy for the study of membrane dynamics and organization in giant unilamellar vesicles, Liposomes: Methods and Protocols, Biological Membrane Models, vol. 2, Humana Press Inc, 2010, pp. 493–508.

[64] L. Pierini, D. Holowka, B. Baird, Fc epsilon RI-mediated association of 6-mu m beads with RBL-2H3 mast cells results in exclusion of signaling proteins from the forming phagosome and abrogation of normal downstream signaling, J. Cell Biol. 134 (1996) 1427–1439.

[65] M. Rusnati, C. Urbinati, E. Tanghetti, P. Dell'Era, H. Lortat-Jacob, M. Presta, Cell membrane GM(1) ganglioside is a functional coreceptor for fibroblast growth factor 2, Proc. Natl. Acad. Sci. U. S. A. 99 (2002) 4367–4372.

[66] I. Leventhal, D. Lingwood, M. Grzybek, U. Coskun, K. Simons, Palmitoylation regulates raft affinity for the majority of integral raft proteins, PNAS 107 (2010) 22050–22054.

[67] S.L. Veatch, S.L. Keller, Miscibility phase diagrams of giant vesicles containing sphingomyelin, Phys. Rev. Lett. 94 (2005).

[68] N. Kahya, D. Scherfeld, P. Schwille, Differential lipid packing abilities and dynamics in giant unilamellar vesicles composed of short-chain saturated glycerol-phospholipids, sphingomyelin and cholesterol, Chem. Phys. Lipids 135 (2005) 169–180.

[69] K. Gaus, T. Zech, T. Harder, Visualizing membrane microdomains by Laurdan 2-photon microscopy (Review), Mol. Membr. Biol. 23 (2006) 41–48.

[70] C. Ringemann, B. Harke, C.V. Middendorff, R. Medda, A. Honigmann, R. Wagner, M. Leutenegger, A. Schoenle, S. Hell, C. Eggeling, Exploring single-molecule dynamics with fluorescence nanoscopy, New J. Phys. 11 (2009) 103054.

[71] S.N. Ahmed, D.A. Brown, E. London, On the origin of sphingolipid/cholesterol-rich detergent-insoluble cell membranes: physiological concentrations of cholesterol and sphingolipid induce formation of a detergent-insoluble, liquid-ordered lipid phase in model membranes, Biochemistry 36 (1997) 10944–10953.

[72] T. Harder, P. Scheiffele, P. Verkade, K. Simons, Lipid domain structure of the plasma membrane revealed by patching of membrane components, J. Cell Biol. 141 (1998) 929–942.

[73] D.M.C. Ramirez, W.W. Ogilvie, L.J. Johnston, NBD-cholesterol probes to track cholesterol distribution in model membranes, Biochim. Biophys. Acta, Biomembr. 1798 (2010) 558–568.

[74] L.A. Bagatolli, To see or not to see: lateral organization of biological membranes and fluorescence microscopy, Biochim. Biophys. Acta, Biomembr. 1758 (2006) 1541–1556.

[75] L.A. Bagatolli, E. Gratton, A correlation between lipid domain shape and binary phospholipid mixture composition in free standing bilayers: a two-photon fluorescence microscopy study, Biophys. J. 79 (2000) 434–447.

[76] H.M. Kim, H.J. Choo, S.Y. Jung, Y.G. Ko, W.H. Park, S.J. Jeon, C.H. Kim, T.H. Joo, B.R. Cho, A two-photon fluorescent probe for lipid raft imaging: C-laurdan, ChemBioChem 8 (2007) 553–559.

[77] H.J. Kaiser, D. Lingwood, I. Leventhal, J.L. Sampaio, L. Kalvodova, L. Rajendran, K. Simons, Order of lipid phases in model and plasma membranes, Proc. Natl. Acad. Sci. U. S. A. 106 (2009) 16645–16650.

[78] O.A. Kucherak, S. Oncul, Z. Darwich, D.A. Yushchenko, Y. Arntz, P. Didier, Y. Mely, A.S. Klymchenko, Switchable Nile red-based probe for cholesterol and lipid order at the outer leaflet of biomembranes, J. Am. Chem. Soc. 132 (2010) 4907–4916.

[79] A. Chattopadhyay, E. London, Parallax method for direct measurement of membrane penetration depth utilizing fluorescence quenching by spin-labeled phospholipids, Biochemistry 26 (1987) 39–45.

[80] D. Lingwood, B. Binnington, T. Rog, I. Vattulainen, M. Grzybek, U. Coskun, C.A. Lingwood, K. Simons, Cholesterol modulates glycolipid conformation and receptor activity, Nat. Chem. Biol. 7 (2011) 260–262.

[81] N. Yahi, A. Aulas, J. Fantini, How cholesterol constrains glycolipid conformation for optimal recognition of Alzheimer's beta amyloid peptide (A beta(1–40)), PLoS One 5 (2010) e9079.

[82] L. Wawrezinieck, H. Rigneault, D. Marguet, P.F. Lenne, Fluorescence correlation spectroscopy diffusion laws to probe the submicron cell membrane organization, Biophys. J. 89 (2005) 4029–4042.

[83] L.A. Bagatolli, J.H. Ipsen, A.C. Simonsen, O.G. Mouritsen, An outlook on organization of lipids in membranes: searching for a realistic connection with the organization of biological membranes, Prog. Lipid Res. 49 (2010) 378–389.

[84] M. Fidorra, A. Garcia, J.H. Ipsen, S. Hartel, L.A. Bagatolli, Lipid domains in giant unilamellar vesicles and their correspondence with equilibrium thermodynamic phases: a quantitative fluorescence microscopy imaging approach, Biochim. Biophys. Acta, Biomembr. 1788 (2009) 2142–2149.

[85] J. Juhasz, F.J. Sharom, J.H. Davis, Quantitative characterization of coexisting phases in DOPC/DPPC/cholesterol mixtures: comparing confocal fluorescence microscopy and deuterium magnetic resonance, Biochim. Biophys. Acta, Biomembr. 1788 (2009) 2541–2552.

[86] E. Sezgin, P. Schwille, K. Simons, I. Leventhal, Elucidating membrane structure and protein behavior using Giant Plasma Membrane Vesicles, Nature Protocols (in press), doi:10.1038/nprot.2012.059.